The Astrophysical Journal Letters, 868:L13 (6pp), 2018 November 20 https://doi.org/10.3847/2041-8213/aaeed6

In Situ Formation of Icy Moons of Uranus and Neptune

Judit Szulágyi[1,2], Marco Cilibrasi[1], and Lucio Mayer[1]
[1] Center for Theoretical Astrophysics and Cosmology, Institute for Computational Science, University of Zurich, Winterthurerstrasse 190, CH-8057 Zurich, Switzerland; judit.szulagyi@uzh.ch
[2] Institute for Particle Physics and Astrophysics, ETH Zurich, Wolfgang-Pauli-Strasse 27, 8093, Zurich, Switzerland
Received 2018 August 10; revised 2018 October 28; accepted 2018 November 5; published 2018 November 19

Abstract

Satellites of giant planets have been thought to form in gaseous circumplanetary disks (CPDs) during the late planet-formation phase, but it was unknown whether or not smaller-mass planets such as the ice giants could form such disks, and thus moons, there. We combined radiative hydrodynamical simulations with satellite population synthesis to investigate the question in the case of Uranus and Neptune. For both ice giants we found that a gaseous CPD is created at the end of their formation. The population synthesis confirmed that Uranian-like, icy, prograde satellite system could form in these CPDs within a couple of 10^5 yr. This means that Neptune could have a Uranian-like moon system originally that was wiped away by the capture of Triton. Furthermore, the current moons of Uranus can be reproduced by our model without the need for planet–planet impact to create a debris disk for the moons to grow. These results highlight that even ice giants—among the most common mass category of exoplanets—can also form satellites, opening a way to a potentially much larger population of exomoons than previously thought.

Key words: accretion, accretion disks – methods: numerical – planets and satellites: formation – planets and satellites: gaseous planets – protoplanetary disks

1. Introduction

Satellites can be found in our solar system, mainly around gas giant planets. As a scaled-down version of planet formation, moons are also assembled within disks, in the gaseous circumplanetary disks (CPD) surrounding the giant planets during their last stage of formation. The larger moons around Jupiter and Saturn are thought to form in gaseous CPDs (Lunine & Stevenson 1982; Pollack & Bodenheimer 1989; Canup & Ward 2009). In contrast, terrestrial planets such as the Earth and Venus have too low of a mass to gather such a disk in the first place, so they can only form an envelope that might turn into a primitive atmosphere (Ormel et al. 2015). The reason why Earth still has a moon is believed to be a result of a planet–planet impact, after which the ejected material formed a debris disk around our planet, where eventually the Moon assembled (Hartmann & Davis 1975; Cameron & Ward 1976). The planetary mass threshold below which gaseous CPD formation—hence satellite formation—cannot occur is still unknown (Ayliffe & Bate 2009).

Past radiative hydrodynamic simulations of CPDs have shown that whether or not a CPD or an envelope forms is not only a question of planetary mass, but also of temperature (Szulágyi et al. 2016, 2017; Szulágyi 2017). These simulations revealed that the cooler the planet (or the surrounding accreting flow), the more likely it is that a disk can form. Satellite formation thus depends on both the planetary mass and the temperature. As planets radiate away their formation heat, they constantly and rapidly cool within the first few million years of their lifetime, therefore whether and when they form a disk is a question of age (and thermal history) as well. Lying between the gas giant and terrestrial planet regime, it was so far unknown whether ice giants like Uranus and Neptune could ever form a gaseous CPD and are therefore capable of forming their satellites there.

Uranus has five major, regular, prograde moons that have nearly circular orbits and low inclinations, which suggests that they formed in a disk (Mosqueira & Estrada 2003). Another model suggested an expanding, tidal disk made of solids (Crida & Charnoz 2012). However, because the planet has an obliquity of 98 degrees, it was assumed that there has been an impact with an Earth-sized object (Safronov 1966; Harris & Ward 1982; Slattery et al. 1992). This impact could have resulted in a debris disk around the planet (similar to the case of Earth) where its moons formed (Dermott 1984; Stevenson 1984; Mousis 2004). The debris disk of the giant impact, however, had to be retrograde (Morbidelli et al. 2012), and the strong impact would evaporate the ice from the ejected debris (Mousis 2004). Therefore, the resulted satellites would be poor in water ice in contrast the observations. The Uranian satellites are in fact made of ∼50% water ice and ∼50% rock. Instead of the major impact scenario, it was suggested that perhaps multiple, smaller impacts caused the tilt and formed a debris disk around the planet (Morbidelli et al. 2012). However, in order to still form prograde satellites, this model requires fine tuning in order to work. Another possibility to tilt Uranus is via secular resonances by a massive moon over a long period of time (Boué & Laskar 2010).

In the case of Neptune, there is only one major moon, Triton, that has 99% of the mass of the entire satellite system. Based on its composition, 157° inclination, and retrograde orbit, Triton is almost certainly a captured Kuiper-belt object (McKinnon et al. 1995). The capture could have dynamically distorted the original satellite system of Neptune, if there was any (Rufu & Canup 2017).

So far, studying satellite formation around Uranus and Neptune was particularly challenging. To address CPD formation realistically, the simulations must have the following two characteristics: (1) sufficiently high resolution to resolve the Hill-sphere, because under-sampling will lead to incorrect physics that will result in envelope formation, and (2) treatment of temperature e.g., with radiation-hydrodynamics, because the temperature in the planet vicinity will also control whether or

not a disk can form (Szulágyi et al. 2016; Cimerman et al. 2017; Szulágyi 2017). So far, there was one hydrodynamics work that attempted to address the CPD formation around Neptune-sized planets, but Wang et al. (2014) did not have any temperature treatment. Particle-based simulations could only address the debris disk hypothesis, which was done by a number of works modeling a potential planet–planet impact (Korycansky et al. 1990; Slattery et al. 1992; Mousis 2004).

In this Letter, we go beyond these previous studies using radiation hydrodynamic simulations with unprecedented resolution in the vicinity of the ice giants. We investigate whether a gaseous CPD could have formed originally around Uranus and Neptune. As a next step, we checked whether or not satellite formation could have occurred in those disks with the use of satellite population synthesis.

2. Methods

2.1. Hydrodynamical Simulations

We ran three-three hydrodynamic simulations for Uranus and Neptune with the JUPITER code (Szulágyi et al. 2016) developed by F. Masset and J. Szulágyi. The code is three-dimensional, grid-based, solving the Euler equations together with radiative dissipation via the flux the limited diffusion approximation method (Kley 1989; Commerçon et al. 2011). In each case there is a spherical coordinate system with a star in the center, surrounded by a gas circumstellar disk. The planets were treated as point masses at the location of the current Uranus (19.2 au) and Neptune (30.1 au). The circumstellar disk radius ranged between 7.7 au and 45.8 au for Uranus, and 12.0 au and 71.8 au for Neptune. Radially 215 cells, azimuthally 618 cells were used on the base mesh. The initial disk opening angle was $5^{\circ}.68$ (from the midplane to the disk surface, using 20 cells), but the disk got thinner after reaching thermal equilibrium with heating and cooling effects. The initial surface density was 16.29 g cm^{-2} at the location of Uranus and 6.63 g cm^{-2} at Neptunes, considering flat disks. This setup corresponds to roughly half of the Minimum Mass Solar Nebula (Hayashi 1981) densities, mimicking the very last stage of planet formation within the solar system when the satellites were formed. Given that real circumstellar disks are dissipating in a nearly exponential fashion at the end of their lifetime, our choice on setting half of the Minimum Mass Solar Nebula was just an educational guess for a mean value that is definitely a mass that the Solar Nebula eventually had at the late stage of its lifetime.

The equation of state in these simulations were of an ideal gas: $p = (\gamma - 1)E_{\rm int}$ connecting the (p) pressure with the internal energy ($E_{\rm int}$) via the adiabatic exponent ($\gamma = 1.43$). The code solves the viscous stress tensor for a constant, kinematic viscosity that is equal to 1.95×10^{14} cm^2 s^{-1} in the case of Uranus and 2.44×10^{14} cm^2 s^{-1} for Neptune. These values corresponds to a reasonable, low alpha-like viscosity that scales with the semimajor axis from the star, which includes that planets form in dead zones. In the simulations the gas can heat up through viscous heating, adiabatic compression and cool through radiative dissipation and adiabatic expansion. The Rosseland-mean-opacities used in the radiation-hydrodynamics simulations were constructed self-consistently from frequency-dependent dust opacities computed with a version of the Mie code from Bohren & Huffman (1984). The dust consisted of 40% water, 40% silicates, and 20% carbonaceous material (Warren 1984; Zubko et al. 1996; Draine 2003), assuming spherical, compact, micron-sized grains. The star was assumed to have solar properties and the dust-to-gas ratio was chosen to be 1%. The opacity table contains the evaporation of the different dust components: 170 K for water, 1500 K for silicates, and 2000 K for carbon, respectively. Above 2000 K the gas opacities were used from Bell & Lin (1994). This method ensures that even though the dust is not treated explicitly in the gas hydrodynamic simulations, its effect on the temperature is taken into account through the dust opacities. The mean molecular weight was set to 2.3 to be consistent with the solar composition.

In order to have sufficient resolution in the CPDs, we increased the resolution in this area with nested meshes. We placed seven additional grids around the ice giants, reaching a final resolution of 1.38×10^{-3} au ($8.1\,R_{\rm p}$) for Uranus and 2.17×10^{-3} au ($13.1\ R_{\rm p}$) for Neptune. For the planets, we fixed their mass, radius, and temperature similarly to Szulágyi (2017). The eight cells around the point masses were the extent of the planet, where the temperatures were fixed to 1000, 500, and 100 K in the three different simulations for Uranus and for Neptune, corresponding to the late surface temperatures of these planets during their formation around 3–4 million years (Fortney & Nettelmann 2010; Nettelmann et al. 2016). This temperature sequence was set in order to mimic how the planet radiates away its formation heat, up until it is fully formed. This is only true in the very late stage of CPD evolution, close to the time when the circumstellar disk has dissipated away.

2.2. Population Synthesis

To examine satellite formation within the CPDs of the hydrodynamical simulations, we used population synthesis. The technique was already successfully used in our previous work (Cilibrasi et al. 2018) for moon formation around Jupiter, hence we only summarize here the main points of our method.

We azimuthally averaged the density and temperature filed on the midplane from the hydrodynamic simulations for the coldest planet case (100 K) when a CPD formed. Satellites can only form in disks, not in envelopes; therefore, we only considered the disk cases. In the semi-analytical model the CPDs have the same properties as in the hydrodynamic simulation: same viscosity, adiabatic index, and mean molecular weight. The angular velocity of the gas, the scale height of the disk, and the sound speed was then computed from the local temperature and density values of the disk and using the common one-dimensional model for disks (Pringle 1981). Due to the fact that the hydrodynamic simulation only computes the gas distribution, we assumed that the dust distribution is the same, but only a fraction of it in mass controlled by the dust-to-gas ratio parameter. The temperature of the dust was assumed to be the same as the gas temperature, assuming perfect thermal equilibrium. The CPD ranged between 1 $R_{\rm p}$ and 500 $R_{\rm p}$, according to the hydrodynamical simulation's CPD radius. The population synthesis includes the CPD evolution (that it cools through radiative dissipation and changes is mass), the continuous mass infall from the circumstellar disk (Szulágyi et al. 2014) as well as the mass loss: accreting to satellites and to the planet. The net mass infall was also computed from the hydrodynamic simulations: $8.4 \times 10^{-8}\,M_{\rm Sun}$ yr^{-1} for Uranus, and $7.4 \times 10^{-8}\,M_{\rm Sun}$ yr^{-1} for Neptune. These infall rates then decreased exponentially, as the circumstellar disk also

dissipates exponentially in the last phase of disk evolution and the feeding to the CPD changes accordingly.

We ran 25,000 individual calculations where in each case varied four parameters.

1. Disk dispersion timescale: different circumstellar disks dissipate on different timescales based on observations, hence we chose to vary this parameter between 0.1 and 1 million years, which is roughly 1/10th of the total lifetime of the circumstellar disk and hence probably of the CPD as well.
2. Dust-to-gas ratio: it has a wide range in circumstellar disks (Ansdell et al. 2016) and according to dust-coagulation studies the CPD can be quite dust rich (Drazkowska & Szulágyi 2018). We therefore varied this parameter between 1% and 50%.
3. Dust-refilling timescale: how quickly the dust is accreted and depleted within the CPD, and how quickly it reaches again its equilibrium profile. This parameter was varied between 100 yr and 1 million years (Cilibrasi et al. 2018).
4. Distance from the planet where the first seeds of satellites are forming. It was varied randomly between 50 and 150 planetary-radius.

At the beginning of simulation, the algorithm creates a new protosatellite with a mass of $10^{-7}\,M_{\rm p}$, which is a seed size that quickly forms from the incoming micron-sized dust via coagulation (Drazkowska & Szulágyi 2018). Then it accretes mass from the dust disk with a common analytical prescription (Greenberg et al. 1991). This accreted mass will be then subtracted from the dust disk density. The protosatellites that form will feel the torque exerted on them by the gas disk and start to migrate. As long as they are small and do not open a gap in the gas distribution of the CPD, they migrate according to the type I regime, computed with the Paardekooper formula (Paardekooper et al. 2010, 2011). In rare cases when they grow to such large mass that can open a gas-gap, they then enter the type II regime of migration and change their orbit on the viscous timescale (Duffell 2015). Sometimes the migration is so fast that the protosatellites will be accreted into the planet. In these cases, we kept track of the lost satellite-mass, in order to know what amount of solids the ice giants were "polluted." The population synthesis simulation stopped when the CPD dissipated, because then the migration of the satellites stopped the and the moon system that formed was considered final.

3. Results

3.1. Uranus

Owing to the high resolution that we could achieve in the planet vicinity within the hydrodynamic simulations, we were able to determine that disks are forming when the planet temperature dropped below 500 K (Figure 1). When steady state of the simulation was reached, the mass of the CPD was only $7.2 \times 10^{-4}\,M_{\rm Uranus}$, measured based on the rotational profile and a corresponding isodensity surface. This is only slightly larger than the integrated mass of the moons ($\sim 10^{-4}\,M_{\rm Uranus}$). However, as it was described earlier, the CPD is not a closed reservoir of mass, it is continuously fed by the circumstellar disk with gas and micron-sized dust (Szulágyi et al. 2014; Fung & Chiang 2016). Some of this mass is accreted to the planet and to the moons, and some is flowing back to the circumstellar disk, maintaining a sort of equilibrium with the circumstellar disk mass (Szulágyi 2017). We measured the net influx rate to the CPDs from the hydrodynamic simulations by defining a box around the CPD and calculating the sum of the inflowing and outflowing gas, finding $8.4 \times 10^{-8}\,M_{\rm Sun}\ {\rm yr}^{-1}$, therefore over the years, there is enough mass flowing through the CPD to eventually build the current satellites of Uranus.

We tested whether or not the CPD with planetary surface temperature of 100 K could form moons with satellite population synthesis. We found that in most cases of the population, there is a satellite system forming. Most of the moons formed over only ~500,000 yr (Figure 2, left panel). While some of the satellites migrated inward in the disk up until they got accreted into the planet, the migration velocities were slow enough, that only 25% of the population was lost. Often sequential satellite formation happened: after the lost satellites new ones could still form until the CPD has dissipated. All of the satellites were formed at a location of the disk where the temperature was below the water freezing point, hence the building blocks of these moons can contain a significant fraction of ices to make icy moons, such as the current ones around Uranus. The masses of the formed satellites spread across several orders of magnitude, mainly in the smaller mass regime between 10^{-7} and $10^{-4}\,M_{\rm Uranus}$ (Figure 2, right panel). On Figure 2 we also mark with red stripes the current masses of the five major satellites. Clearly, the moon system of Uranus as we see today can be reproduced by our model. In 5.8% of the cases we can see systems with four or five satellites and with a total mass between 0.5 and 2 times the current Uranian satellites. Considering the distances from the central planet, we found that in about 18% of the cases they are comparable to the orbital radii of the current five Uranian satellites. Both conditions together occur in 5.1% of all the cases.

We investigated the impact of different physical ingredients in the model by varying only one parameter at a time. We found that the masses of the final moons basically scales linearly with the dust-to-gas ratio, hence in order to reproduce the major five satellites, a dust-to-gas ratio of 7% or higher is needed within the CPD. Moreover, the dust-refilling timescale has to be 10,000 yr or shorter, meaning relatively quick dust evolution, which can easily happen according to a recent study of dust-coagulation in CPDs (Drazkowska & Szulágyi 2018).

Tests were made also on the distance where the satellite seeds were formed. In this case, when we fixed one location in the disk where satellites can form (e.g., at $50M_{\rm Uranus}$, at $100M_{\rm Uranus}$, and at $150M_{\rm Uranus}$), we found the number of survived satellites are larger when the seeds were all placed at $150M_{\rm Uranus}$ than at $50M_{\rm Uranus}$. This is just because excluding the outer CPD will of course result in more compact moon system that can accommodate fewer satellites. Because one has no a priori knowledge on where the current satellites were formed, we randomized the satellite-seed positions in our model presented in this Letter.

3.2. Neptune

As in the case of Uranus, the nearly equal-mass Neptune could also form a CPD when $T_{\rm p} < 500$ K (Figure 1). The CPD in this case was $1.7 \times 10^{-3}\,M_{\rm Neptune}$. The mass infall rate to the CPD was found to be $7.4 \times 10^{-8}\,M_{\rm Sun}\ {\rm yr}^{-1}$.

From the population synthesis, we found similar trends for Neptune as in the case of Uranus. This CPD could also form

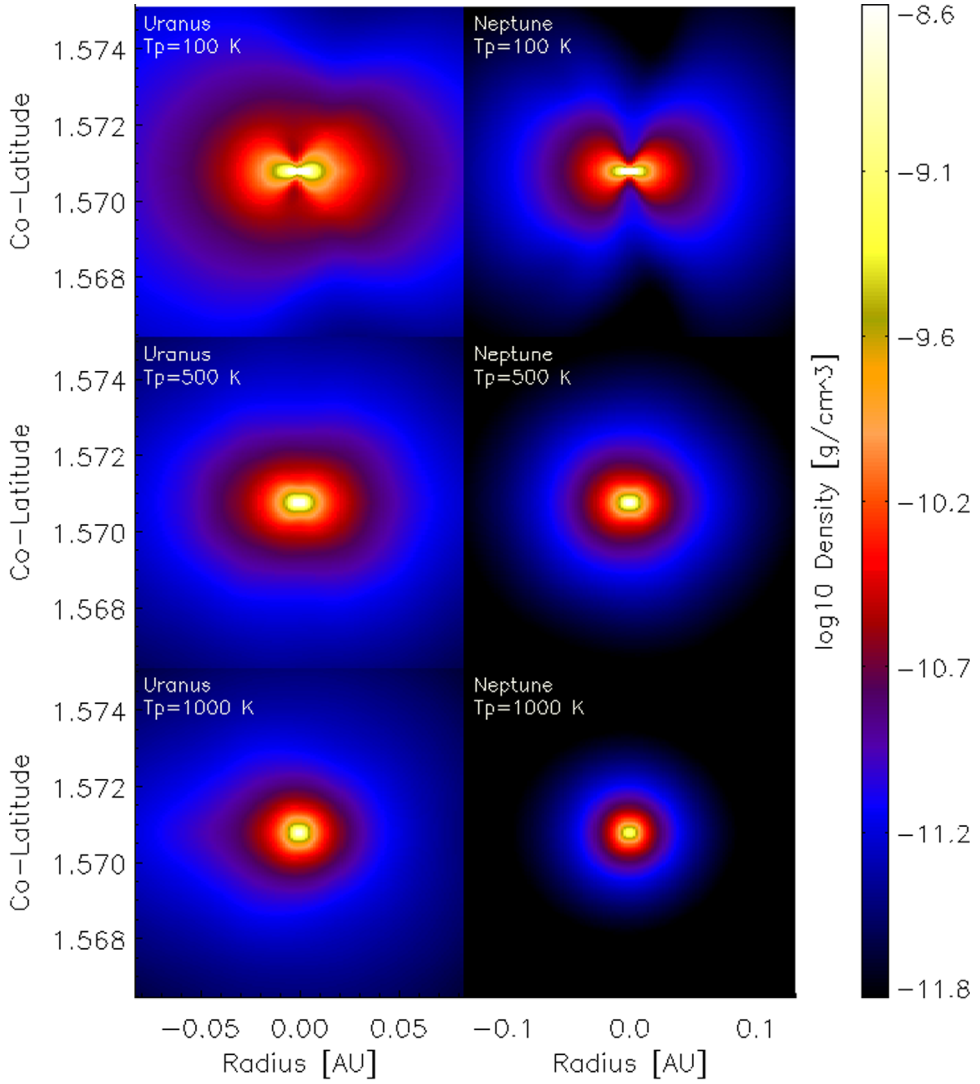

Figure 1. Zoom to the circumplanetary disk around Uranus (left column) and Neptune (right column). The different rows of the density maps correspond to various planetary surface temperatures mimicking the late stages of ice giant formation when these planets were rapidly cooling.

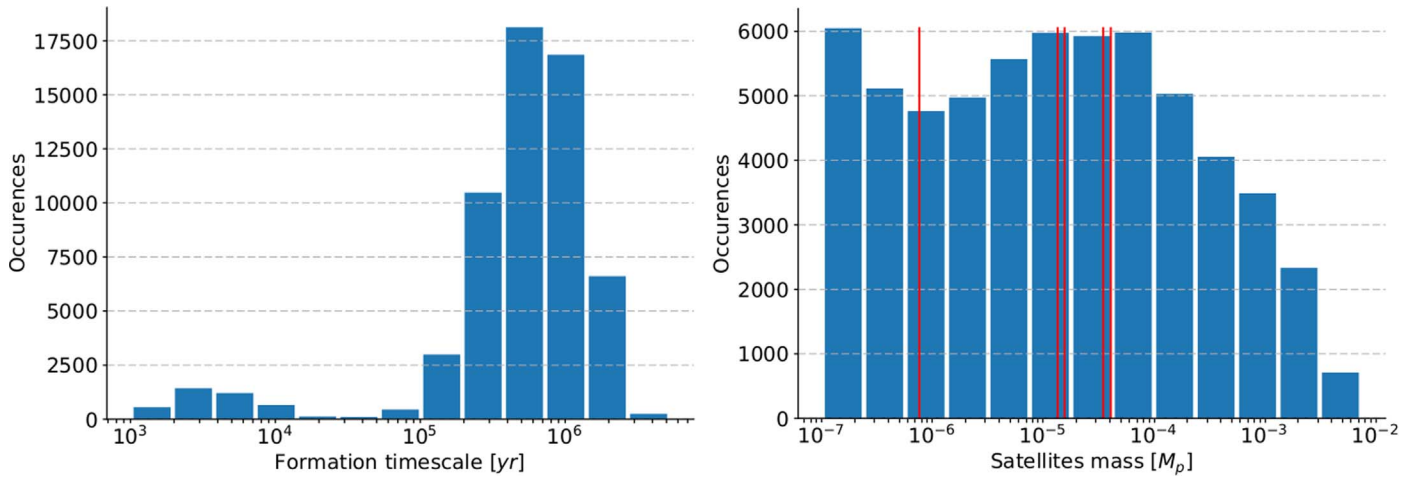

Figure 2. Left panel: formation timescales of the moons around Uranus in our population synthesis. Right panel: mass distribution of the formed satellite population around Uranus, where the red lines represent its current, major five moons.

relatively massive moons in most of the cases. The majority of the population formed over a couple of 10^5 yr (Figure 3, left panel). The entire CPD had a temperature below water freezing point, so this disk also likely forms only icy satellites. The masses of the formed moons were again often in the low-mass regime between 10^{-7} and 10^{-4} $M_{\rm Neptune}$, i.e., smaller than the

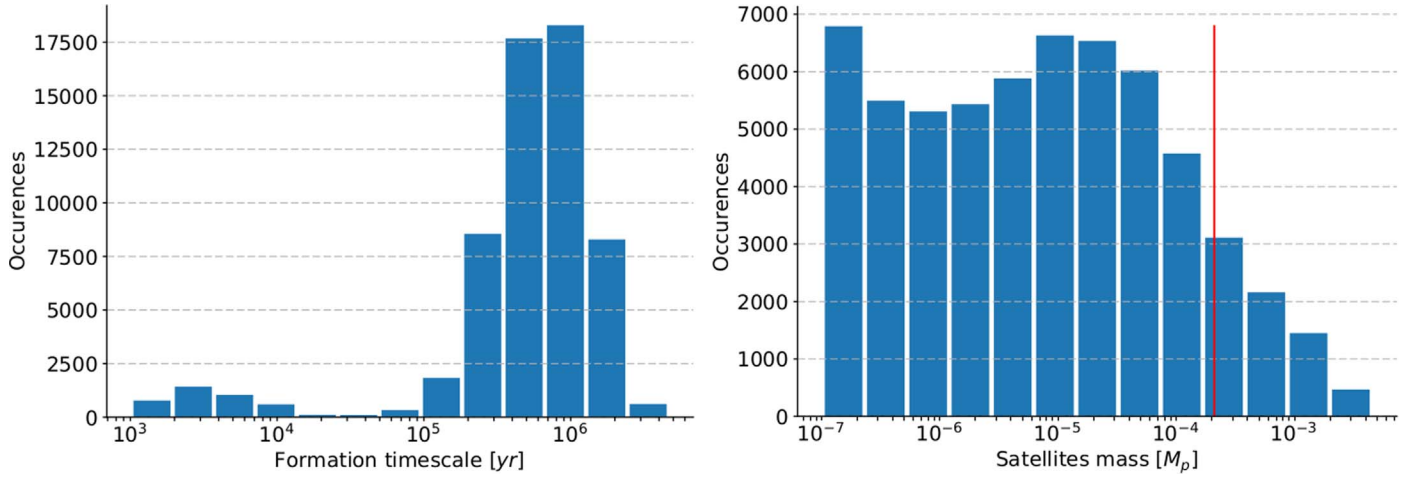

Figure 3. Left: formation timescales of the moons around Neptune in our population synthesis. Right: mass distribution of the formed satellite population around Neptune, where the red line shows the mass of its current one major moon, Triton.

mass of Triton (Figure 3, right panel). Note that Triton is most likely a captured Kuiper-object (McKinnon et al. 1995), so it did not form around Neptune; our mass comparison in this case is simply for scaling purposes. However, our result is that a similar moon system could have formed around Neptune like around Uranus, before the capture of Triton happened. It was already suggested by a dynamical study (Rufu & Canup 2017) that the capture of Triton is only possible, if the original moon system was similar in mass than the Uranian satellite system.

4. Conclusion and Discussion

We investigated CPD formation and moon formation around Uranus and Neptune with combining radiative hydrodynamical simulations with satellite population synthesis. We found that both Uranus and Neptune could form a gaseous disk at the end of their formation, when their surface temperature dropped below 500 K. These disks are able to form satellites in them within a few hundred-thousand years. The masses of such satellite-systems for both planets were often similar to the current one around Uranus. All of the formed moons must be icy in composition, given that they formed in a CPD that has a temperature below water freezing point. We highlighted that Neptune could have originally had a similar satellite system that we see today around Uranus, which was perturbed and got lost by the capture of Triton from the Kuiper-belt, as the dynamical study of Rufu & Canup (2017) suggested before.

Given that here we showed that the moons of Uranus could have formed in the gaseous CPD around the ice giant, there is no need for a planet–planet impact. Our satellite formation model works for Uranus, no matter whether the axial tilt of the planet was caused by multiple smaller impacts before the satellites formed (Morbidelli et al. 2012), or by secular resonance with a larger-mass moon (Boué & Laskar 2010), that we can even form within our CPD. Unlike the impact scenarios, our gaseous disk naturally forms icy, prograde moons without the need of fine tuning.

As it is possible to form satellites around ice giants, satellite formation seems to be more frequent than it was previously thought. This is particularly exciting for exomoon-hunting because Neptune-mass exoplanets are among the most common mass category of exoplanets; if they can also form satellites, there must be a much larger population of exomoons than previously considered. Moreover, icy moons in our solar system are the main targets to search for extraterrestrial life (Europa in case of Jupiter; Greenberg 2011; Sparks et al. 2017; and Enceladus in case of Saturn; Parkinson et al. 2008), hence a larger amount of icy satellites of a similar kind means a potentially larger sample of habitable words.

We thank the anonymous referee for useful suggestions that improved this manuscript. This work was funded by the Swiss National Science Foundation (SNSF) Ambizione grant PZ00P2_174115. The simulations were done on the "Moench" cluster hosted at the Swiss National Computational Centre.

ORCID iDs

Judit Szulágyi https://orcid.org/0000-0001-8442-4043

References

Ansdell, M., Williams, J. P., van der Marel, N., et al. 2016, ApJ, 828, 46
Ayliffe, B. A., & Bate, M. R. 2009, MNRAS, 397, 657
Bell, K. R., & Lin, D. N. C. 1994, ApJ, 427, 987
Bohren, C. F., & Huffman, D. R. 1984, Natur, 307, 575
Boué, G., & Laskar, J. 2010, ApJL, 712, L44
Cameron, A. G. W., & Ward, W. R. 1976, LPSC, 7, 120
Canup, R. M., & Ward, W. R. 2009, in Europa, ed. R. T. Pappalardo et al. (Tucson, AZ: Univ. Arizona Press), 59
Cilibrasi, M., Szulágyi, J., Mayer, L., et al. 2018, MNRAS, 480, 4355
Cimerman, N. P., Kuiper, R., & Ormel, C. W. 2017, MNRAS, 471, 4662
Commerçon, B., Teyssier, R., Audit, E., et al. 2011, A&A, 529, A35
Crida, A., & Charnoz, S. 2012, Sci, 338, 1196
Dermott, S. F. 1984, in NASA Conf. Pub. 2330, Uranus and Neptune, ed. J. T. Bergstralh (Pasadena, CA: NASA), 377
Draine, B. T. 2003, ARA&A, 41, 241
Drazkowska, J., & Szulágyi, J. 2018, arXiv:1807.02638
Duffell, P. C. 2015, ApJL, 807, L11
Fortney, J. J., & Nettelmann, N. 2010, SSRv, 152, 423
Fung, J., & Chiang, E. 2016, ApJ, 832, 105
Greenberg, R. 2011, AsBio, 11, 183
Greenberg, R., Bottke, W. F., Carusi, A., et al. 1991, Icar, 94, 98
Harris, A. W., & Ward, W. R. 1982, AREPS, 10, 61
Hartmann, W. K., & Davis, D. R. 1975, Icar, 24, 504
Hayashi, C. 1981, PThPS, 70, 35
Kley, W. 1989, A&A, 208, 98
Korycansky, D. G., Bodenheimer, P., Cassen, P., et al. 1990, Icar, 84, 528
Lunine, J. I., & Stevenson, D. J. 1982, Icar, 52, 14
McKinnon, W. B., Lunine, J. I., & Banfield, D. 1995, Neptune and Triton (Tucson, AZ: Univ. Arizona Press)
Morbidelli, A., Tsiganis, K., Batygin, K., et al. 2012, Icar, 219, 737

Mosqueira, I., & Estrada, P. R. 2003, Icar, 163, 198
Mousis, O. 2004, A&A, 413, 373
Nettelmann, N., Wang, K., Fortney, J. J., et al. 2016, Icar, 275, 107
Ormel, C. W., Shi, J.-M., & Kuiper, R. 2015, MNRAS, 447, 3512
Paardekooper, S.-J., Baruteau, C., Crida, A., et al. 2010, MNRAS, 401, 1950
Paardekooper, S.-J., Baruteau, C., & Kley, W. 2011, MNRAS, 410, 293
Parkinson, C. D., Liang, M.-C., Yung, Y. L., & Kirschivnk, J. L. 2008, OLEB, 38, 355
Pollack, J. B., & Bodenheimer, P. 1989, in Origin and Evolution of Planetary and Satellite Atmospheres, ed. S. K. Atreya et al. (Tucson, AZ: Univ. Arizona Press), 564
Pringle, J. E. 1981, ARA&A, 19, 137
Rufu, R., & Canup, R. M. 2017, AJ, 154, 208
Safronov, V. S. 1966, SvA, 9, 987
Slattery, W. L., Benz, W., & Cameron, A. G. W. 1992, Icar, 99, 167
Sparks, W. B., Schmidt, B. E., McGrath, M. A., et al. 2017, ApJL, 839, L18
Stevenson, D. J. 1984, W&SO, 3, 1
Szulágyi, J. 2017, ApJ, 842, 103
Szulágyi, J., Masset, F., Lega, E., et al. 2016, MNRAS, 460, 2853
Szulágyi, J., Mayer, L., & Quinn, T. 2017, MNRAS, 464, 3158
Szulágyi, J., Morbidelli, A., Crida, A., et al. 2014, ApJ, 782, 65
Wang, H.-H., Bu, D., Shang, H., et al. 2014, ApJ, 790, 32
Warren, S. G. 1984, ApOpt, 23, 1206
Zubko, V. G., Mennella, V., Colangeli, L., & Bussoletti, E. 1996, MNRAS, 282, 1321